Aquaglyceroporin AQP9: Solute permeation and metabolic control of expression in liver

Jennifer M. Carbrey*†, Daniel A. Gorelick-Feldman*†, David Kozono*, Jeppe Praetorius‡, Søren Nielsen‡, and Peter Agre*§¶

Departments of *Biological Chemistry and §Medicine, Johns Hopkins School of Medicine, Baltimore, MD 21205; and ‡Water and Salt Research Center, University of Aarhus, DK-8000 Aarhus, Denmark

Contributed by Peter Agre, December 30, 2002

Aquaglyceroporins form the subset of the aquaporin water channel family that is permeable to glycerol and certain small, uncharged solutes. AQP9 has unusually broad solute permeability and is expressed in hepatocyte plasma membranes. Proteoliposomes reconstituted with expressed, purified rat AQP9 protein were compared with simple liposomes for solute permeability. At pH 7.5, AQP9 proteoliposomes exhibited Hg^{2+}-inhibitible glycerol and urea permeabilities that were increased 63-fold and 90-fold over background. β-Hydroxybutyrate permeability was not increased above background, and osmotic water permeability was only minimally elevated. During starvation, the liver takes up glycerol for gluconeogenesis. Expression of AQP9 in liver was induced up to 20-fold in rats fasted for 24–96 h, and the AQP9 level gradually declined after refeeding. No changes in liver AQP9 levels were observed in rats fed ketogenic diets or high-protein diets, but AQP9 levels were elevated in livers of rats made diabetic by streptozotocin injection. When blood glucose levels of the diabetic rats were restored to normal by insulin treatments, the AQP9 levels returned to baseline. Confocal immunofluorescence revealed AQP9 immunostaining on the sinusoidal surfaces of hepatocyte plates throughout the livers of control rats. Denser immunostaining was observed in the same distribution in livers of fasted and streptozotocin-treated rats. We conclude that AQP9 serves as membrane channel in hepatocytes for glycerol and urea at physiological pH, but not for β-hydroxybutyrate. In addition, levels of AQP9 expression fluctuate depending on the nutritional status of the subject and the circulating insulin levels.

The AQP9 cDNA was first isolated during efforts to clone urea transporters by expression in oocytes (1). Expressed in testes, leukocytes, and brain, AQP9 is abundant in liver (1) where it resides in hepatocyte plasma membranes facing the sinusoids (2–4). The coding sequence of AQP9 is more closely related to AQP3 (5) and AQP7 (6), which are both permeated by glycerol and water. This subset of proteins, referred to as aquaglyceroporins, is functionally distinct from the water-selective homologs AQP1, AQP2, AQP4, and AQP5 (7). The original studies of *Xenopus laevis* oocytes expressing rat AQP9 reported permeability to a wide range of ^{14}C- or ^{3}H-labeled solutes including polyols, carbamides, purines, pyrimidines, nucleosides, and monocarboxylates (1). Glycerol and urea permeability have been confirmed with AQP9 oocytes (8), but studies of proteoliposomes reconstituted with purified AQP9 protein have not been reported.

The physiological functions of AQP9 are uncertain. During prolonged fasting, glycerol released from adipocytes via AQP7 may be taken up by the liver via AQP9 for gluconeogenesis. Urea, a byproduct of amino acid deamination, and β-hydroxybutyrate, an alternative fuel, may be released from liver via AQP9. An elegant series of recent studies of adipocyte AQP7 and liver AQP9 mRNAs and promoters suggested that the genes are coordinately regulated during fasting and type 1 diabetes mellitus (9), but this has not been confirmed with studies of the AQP7 and AQP9 proteins.

We undertook studies to define the permeation of proteoliposomes reconstituted with purified rat AQP9 protein and to provide evidence that expression of AQP9 protein is altered in rats during fasting and insulin deficiency. Our studies indicate that AQP9 facilitates hepatocyte glycerol influx and urea efflux, establishing a greater functional repertoire for AQP9 as a solute channel with minor water transport capacity.

Materials and Methods

Plasmid Construction. Standard methods were used (10). pXβG-ev1-AQP9 was constructed with AQP9 cDNA prepared from rat liver total RNA and inserted into the *Bgl*II site of pXβG-ev1 (11). pYES2-AQP9 was made from pXβG-ev1-AQP9 with rat AQP9 amplified with primers 5′EcoRA9 (5′-AGAAACGAATTCATGCCTTCTGAGAAGGAC-3′) and 3′XbaRA9 (5′-CTGGCCTCTAGACTACATGATGACACTGAG-3′). The product contained an *Eco*RI site at the 5′ end and an *Xba*I site at the 3′ end. pYES2 vector (Invitrogen) encoding MGHHHHHHHHHSSGHIEGRHEF between the *Hin*dIII and *Eco*RI sites was digested with *Eco*RI and *Xba*I for ligation with AQP9.

Expression and Purification of AQP9. Rat AQP9 was purified from protease-deficient (*pep4*Δ) *Saccharomyces cerevisiae* expressing pYES2-AQP9 (12, 13). Membranes were solubilized in 200 ml of buffer A [100 mM K_2HPO_4/10% glycerol/200 mM NaCl/5 mM 2-mercaptoethanol/3% octyl glucoside (*N*-octyl-β-D-glucopyranoside, Calbiochem) and protease inhibitors (EDTA-free complete protease inhibitor mixture tablets, Roche Biochemicals)] and loaded on an Ni-NTA agarose column (nickel-charged nitrilotriacetic acid, Qiagen, Valencia, CA), washed, and then eluted with buffer A containing 100 mM and 600 mM imidazole.

AQP9 Proteoliposome Transport Studies. Purified AQP9 protein was reconstituted with *Escherichia coli* polar lipid extract (Avanti, Alabaster, AL) into proteoliposomes by dialysis at a lipid to protein ratio of ≈100:1 overnight at 4°C vs. 100 volumes of reconstitution buffer [RB; 50 mM Mops/150 mM *N*-methyl-D-glucamine (Calbiochem)/1 mM NaN_3 (Sigma) and protease inhibitors (EDTA-free), pH 7.5] (12, 13).

AQP9 proteoliposomes and protein-free control liposomes were analyzed by light scattering using a stopped-flow apparatus (SF-2001, Kin Tek Instruments, University Park, PA) with a dead time of ≤1 ms. Osmotic water permeability of proteoliposomes was measured at 4°C as described (13). Glycerol, urea, and β-hydroxybutyrate permeability were measured with proteoliposomes preequilibrated with solutes >15 min on ice, and permeability was measured at 24°C as described (13). Some proteoliposomes were reconstituted by dialysis in the presence of DL-β-hydroxybutyrate (total osmolality 855 mosM). Second-order rate constants were calculated; the first constant represents AQP9 transport and the second represents background permeability.

†J.M.C. and D.A.G.-F. contributed equally to this work.

¶To whom correspondence should be addressed. E-mail: pagre@jhmi.edu.

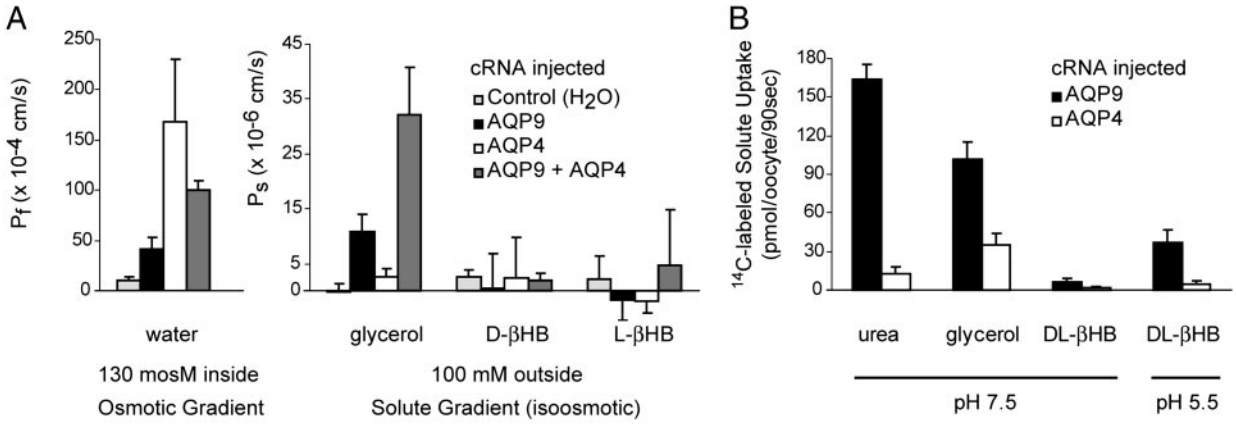

Fig. 1. Solute permeability measurements of rat AQP9 or rat AQP4 in oocytes. *X. laevis* oocytes were injected with 5 ng of rat AQP9 cRNA, 5 ng of rat AQP4 (M23) cRNA, 2.5 ng of AQP4 plus 2.5 ng of AQP9 cRNA, or 50 nl of water and cultured for 3 days. (*A*) Osmotic water permeability (P_f) was assayed by transferring oocytes from 200 to 70 mosM Barth's solution, and swelling was monitored by videomicroscopy. Solute permeability was assayed by placing oocytes in isotonic solution containing 100 mM indicated solute. The concentration gradient caused solute influx resulting in water influx and oocyte swelling. Data are mean ± SD from six oocytes. (*B*) Uptake of ^{14}C-labeled solute was measured over 90 s at room temperature. Values represent mean ± SD from 6–10 oocytes.

Oocyte Transport Studies. Capped cRNAs were synthesized *in vitro* from linearized pXβG-ev1 plasmids (11). Defolliculated *X. laevis* oocytes were injected with 5 ng of cRNA or 50 nl of diethyl pyrocarbonate-treated water. Injected oocytes were incubated for 3 days at 18°C in 200 mosM modified Barth's solution. Osmotic water permeability (11) and ^{14}C-labeled solute permeability methods were used (1). Nonisotopic solute permeabilities (P_s) were measured by placing oocytes in 200 mosM modified Barth's solution containing 100 mosM of solute, causing water influx and oocyte swelling. P_s was calculated from the oocyte surface area ($S = 0.045$ cm^2), initial oocyte volume ($V_o = 9 \times 10^{-4}$ cm^3), the initial slope of the relative volume increase $d(V/V_o)/dt$, the total osmolality of the system ($osm_{total} = 200$ mosM), and the osmotic solute gradient ($sol_{out} - sol_{in}$) as follows: $P_s = [osm_{total} \times V_o \times d(V/V_o)/dt]/[S \times (sol_{out} - sol_{in})]$.

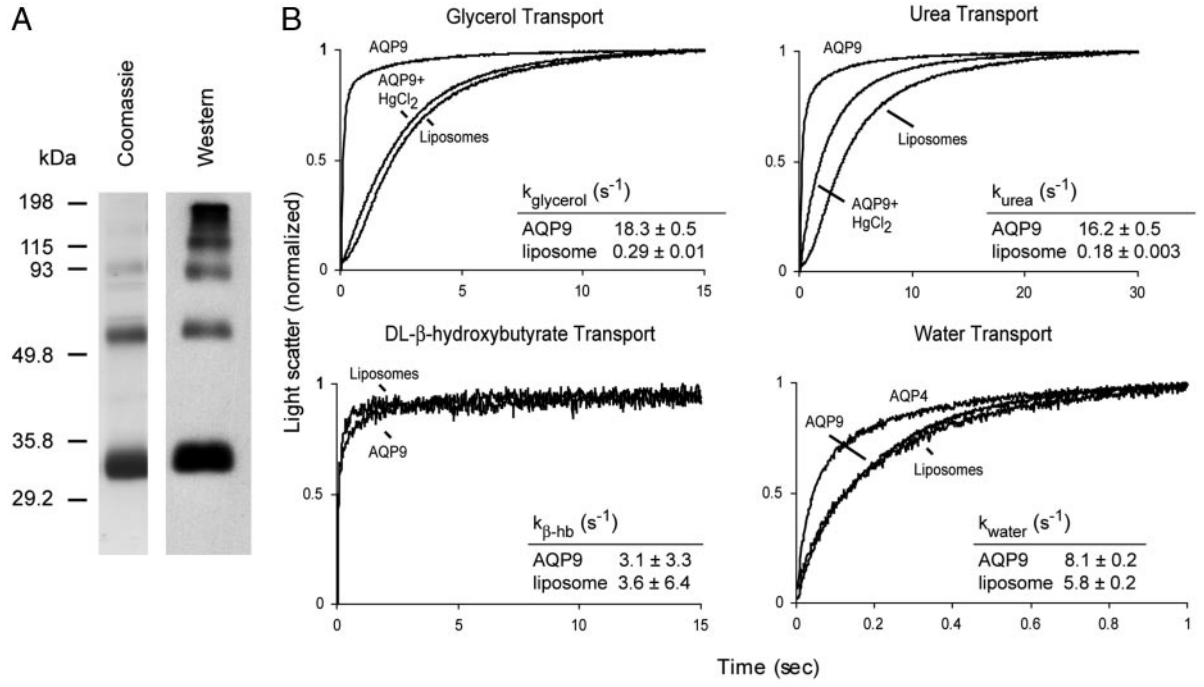

Fig. 2. Purification of rat AQP9 protein and measurement of solute transport in AQP9 proteoliposomes. (*A*) Coomassie-stained SDS/polyacrylamide gel (*Left*) and anti-AQP9 immunoblot (*Right*) of purified AQP9 protein. (*B*) Permeability of AQP9 proteoliposomes (reconstituted from pure *E. coli* lipids and purified AQP9 protein) or control liposomes (reconstituted with no protein) were evaluated for permeability for glycerol, urea, DL-β-hydroxybutyrate, or water. For solute transport measurement, proteoliposomes or liposomes containing the indicated solute were rapidly mixed with an equal volume of isotonic solution containing sucrose as a nonpermeant osmolyte. The concentration gradient caused solute efflux resulting in osmotically driven water efflux and vesicle shrinkage measured by light scattering. To measure inhibition of solute transport, proteoliposomes were incubated with 1 mM $HgCl_2$ at least 15 min before measuring light scattering. For water transport measurement, AQP9 proteoliposomes, AQP4 proteoliposomes, and control liposomes were subjected to an abrupt 50% increase in extravesicular osmolality resulting in water efflux, and shrinking was measured by light scattering. The kinetics of 10 measurements were normalized and fitted to a characteristic first- or second-order exponential equation dependent on the time course of water efflux.

Animal Studies. Experimental protocols were approved by the Institutional Animal Care and Use Committee and conform to National Institutes of Health guidelines. Male 225- to 250-g Sprague–Dawley rats (Taconic) in individual cages with free access to water received standard rodent chow, 14% protein, and 6% fat (5P07, Purina); ketogenic diet, 91% fat and 9% protein (96355, Harlan Teklad) (14); or 60% protein diet (5787, Purina). Some rats were injected s.c. with human insulin (Sigma) at 5 units/kg. Streptozotocin (30 mg/ml, Sigma) in 50 mM NaCitrate (pH 4.5) was injected i.p. at 100 mg/kg into other rats; some were injected s.c. with 13 units/kg NPH insulin (Humulin N, Eli Lilly) at 0900 and 1800 hours. Rats were killed at 1300 hours. Glucose, urea nitrogen, and β-hydroxybutyrate concentrations were measured in serum (Sigma kits). Blood glucose was measured with a OneTouch Ultra Blood glucose monitoring system (Lifescan, Mountain View, CA).

Tissue Processing, Immunoblotting, and Microscopy. Tissues were immediately placed on ice and homogenized, and membranes were collected by centrifugation (15); 25 μg of membrane protein was analyzed by SDS/PAGE (16); immunoblots were reacted with 3.5 μg/ml rabbit anti-rat AQP9 (Chemicon). Sample loadings were confirmed with Ponceau S (Sigma), and band intensities were scanned with a MacBAS bioimaging analyzer system (Fuji).

Control rats, rats fasted 4 days, or rats injected with streptozotocin 9 days earlier were perfusion-fixed with 3% paraformaldehyde, in 0.1 M cacodylate buffer, via left ventricle and prepared for paraffin embedding and immunohistochemistry (17). Confocal laser microscopy (Leica DMRS) was performed by using rabbit anti-rat AQP9 (Alpha Diagnostics) and goat anti-rabbit secondary antibodies (Alexa 488, Molecular Probes), and the images were merged with differential interference contrast images.

Results

Permeability of AQP9 in Oocytes. *X. laevis* oocytes injected with cRNAs encoding rat AQP9, AQP4, or both were compared with oocytes injected with 50 nl of water. Coefficients of osmotic water permeability (P_f) were determined from rates of swelling after transfer from 200 to 70 mosM Barth's solution. Water-injected oocytes exhibited low water permeability, whereas the P_f of AQP9 oocytes was increased ≈4-fold, AQP4 oocytes ≈20-fold, and AQP9 + AQP4 oocytes ≈12-fold (Fig. 1*A Left*).

Coefficients of P_s were determined by measuring oocyte swelling after transfer to isoosmotic Barth's solution containing 100 mosM solute (glycerol, D- or L-β-hydroxybutyrate). Water-injected oocytes failed to swell after transfer to glycerol, and AQP4 oocytes exhibited minimal permeability (Fig. 1*A Right*). AQP9 oocytes exhibited increased glycerol permeability, but permeability of the AQP9 + AQP4 oocytes was 2-fold higher. This synergistic response is presumed to represent rapid glycerol influx through AQP9 followed by rapid water influx through AQP4. D- and L-β-hydroxybutyrate permeabilities were too low to measure accurately.

Solute permeabilities were also determined by measuring ^{14}C-labeled solute uptake. At neutral pH, AQP9 oocytes exhibited much higher permeability to ^{14}C-urea and ^{14}C-glycerol than AQP4 oocytes (Fig. 1*B*). At pH 7.5, the permeability of AQP9 oocytes to the racemic mixture DL-^{14}C-β-hydroxybutyrate was too low to measure accurately. At pH 5.5, the permeability of AQP9 oocytes for DL-^{14}C-β-hydroxybutyrate was 10 times higher than the AQP4 oocytes (Fig. 1*B*).

Permeability of AQP9 in Proteoliposomes. Oocytes express endogenous membrane proteins, so a defined system was used to measure permeability of purified AQP9 protein. Rat AQP9 with a polyhistidine tag at the N terminus was expressed in *S. cerevisiae* and purified. Coomassie staining and immunoblotting of SDS/PAGE showed a major band at ≈32 kDa and a ladder of oligomers (Fig. 2*A*). Purified AQP9 and pure *E. coli* lipids were reconstituted into resealed proteoliposomes for comparison with control liposomes reconstituted from lipid without protein.

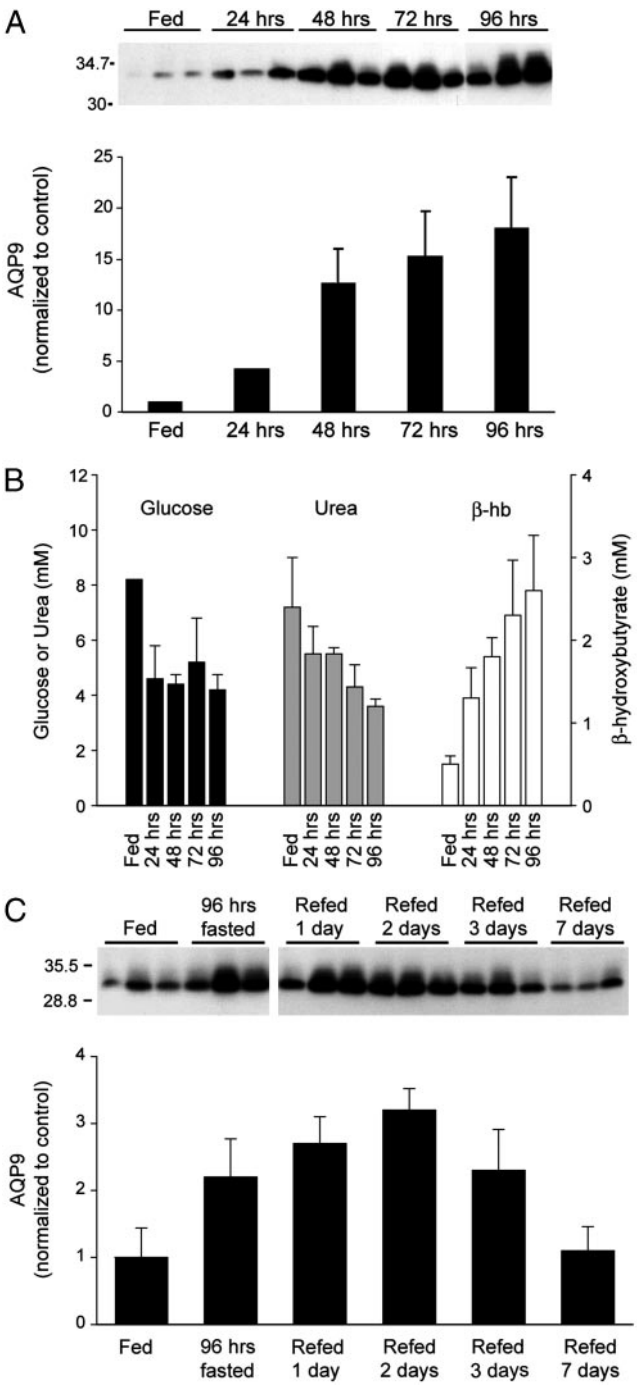

Fig. 3. Effect of fasting and refeeding on AQP9 levels in liver. (*A Upper*) Anti-AQP9 immunoblot of liver membranes from three rats after the indicated time of fasting. (*A Lower*) Scanning densities of anti-AQP9 immunoblot. (*B*) Average serum levels of glucose, urea, and β-hydroxybutyrate from the same rats. (*C*) After 96 h of fasting, rats were allowed access to food. (*Upper*) Anti-AQP9 immunoblot of liver membranes from three rats after indicated time of refeeding. (*Lower*) Scanning densities of anti-AQP9 immunoblot. Values represent mean ± SD from three rats.

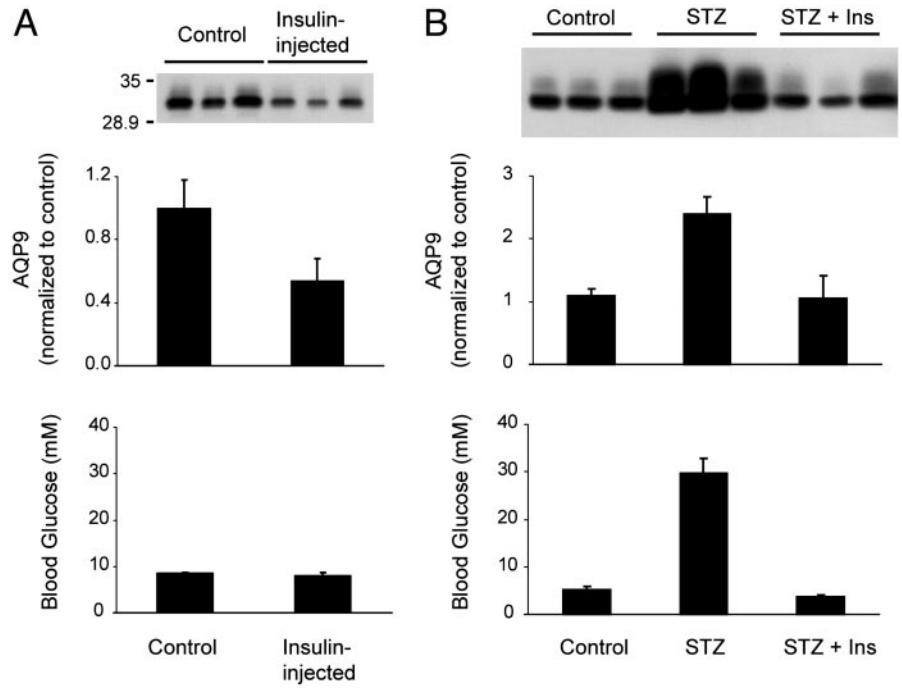

Fig. 4. Effect of insulin on AQP9 levels in liver. (*A*) Insulin injection. (*Top*) Anti-AQP9 immunoblot of liver membranes from three rats killed 24 h after injection of buffer or 5 units/kg regular insulin, as indicated. (*Middle*) Scanning densities of anti-AQP9 immunoblot. (*Bottom*) Average blood levels of glucose at death. (*B*) Streptozotocin pretreatment followed by insulin injection. (*Top*) Anti-AQP9 immunoblot of liver membranes from three rats killed 9 days after injection of buffer (control), 100 mg/kg streptozotocin (STZ), or streptozotocin followed by 4 days of bidaily injections of 13 units/kg NPH insulin (STZ + ins). (*Middle*) Scanning densities of anti-AQP9 immunoblot. (*Bottom*) Average blood levels of glucose at death. Values represent mean ± SD from three rats.

AQP9 proteoliposomes loaded with glycerol, urea, or DL-β-hydroxybutyrate were rapidly transferred by stopped-flow to isoosmotic fluid containing sucrose as a nonpermeant osmolyte. Permeable membranes release solute, causing water efflux measurable by light scattering. Glycerol permeability of AQP9 proteoliposomes was 63 times higher than liposomes and was almost entirely blocked with 1 mM $HgCl_2$ (Fig. 2*B*); urea permeability of AQP9 proteoliposomes was 90 times higher than liposomes. When exposed to a simple osmotic gradient, AQP9 proteoliposomes were only 1.4 times as permeable as liposomes. At neutral pH, DL-β-hydroxybutyrate permeability of AQP9 proteoliposomes and liposomes was equivalent (Fig. 2*B*), even if the proteoliposomes were reconstituted in the presence of DL-β-hydroxybutyrate. Precipitations appeared when DL-β-hydroxybutyrate permeability measurements were attempted at pH 5.5 (not shown).

AQP9 Expression in Liver. AQP9 protein levels were increased in liver of rats within 12 h of fasting (not shown). Continued fasting for up to 96 h with free access to water caused incremental increases in AQP9 levels (Fig. 3*A*). During this time, the average glucose and urea concentrations decreased by approximately half, whereas β-hydroxybutyrate increased 4-fold (Fig. 3*B*). Liver AQP9 levels increased in all five of our experiments, rising as high as 20-fold above baseline. When rats fasted 96 h were refed, levels of AQP9 in liver gradually declined after 3 days and returned to baseline levels after 1 week (Fig. 3*C*).

Ketogenic and high protein diets did not alter liver AQP9 levels. Ketogenic diets increase serum concentrations of β-hydroxybutyrate (14), but after a week rats did not exhibit changes in liver AQP9 despite a 20-fold increase in serum β-hydroxybutyrate (not shown). Rats fed a high protein diet for a week did not exhibit changes in liver AQP9, despite a 4-fold increase in serum urea (not shown).

Effects of Insulin on AQP9 Expression in Liver. A single injection of 5 units/kg regular insulin (rapid-acting) caused a reduction in AQP9 in liver after 24 h (Fig. 4*A*). To evaluate the chronic effects of insulin, rats were injected with 100 mg/kg streptozotocin to destroy pancreatic β-cells; control rats were injected with buffer. After 5 days, the streptozotocin-treated rats were divided into two groups: one group was injected twice daily with 13 units/kg NPH insulin (long-acting) for 4 days; the other group received no injections. By 5 days, the streptozotocin-injected rats were all frankly diabetic, and by 9 days serum glucose levels were ≈8-fold higher than control rats, whereas serum glucose levels were normal in streptozotocin-injected rats treated with insulin (Fig. 4*B*). AQP9 expression in liver was increased >2-fold in the livers of streptozotocin-injected rats when compared with livers from control rats or streptozotocin-injected rats treated with insulin (Fig. 4*B*). Changes in liver AQP9 expression were not observed in rats injected s.c. with 3 mg/kg dexamethasone or 450 μg/kg glucagon when compared with control buffer-injected rats (data not shown).

Confocal Immunofluorescence Microscopy of AQP9 in Liver. Consistent with previous studies (2–4), distinct AQP9 immunolabeling was observed exclusively in plasma membranes at the sinusoidal surfaces of hepatocyte plates of livers from control rats (Fig. 5*A*). The overall distribution of AQP9 was similar in livers of fasted animals, although the level of immunolabeling was dramatically increased throughout the lobules (Fig. 5*B*). Furthermore, weak staining of nonsinusoidal surfaces was observed, and hepatocytes were of markedly smaller size. Similar changes were observed after streptozotocin treatment (Fig. 5*C*).

Discussion

Because of potential physiological importance, we investigated transport of water, glycerol, urea, and β-hydroxybutyrate by AQP9 (Fig. 1). Osmotic swelling assays in oocytes showed that rat AQP9 transports water much less rapidly than a water-

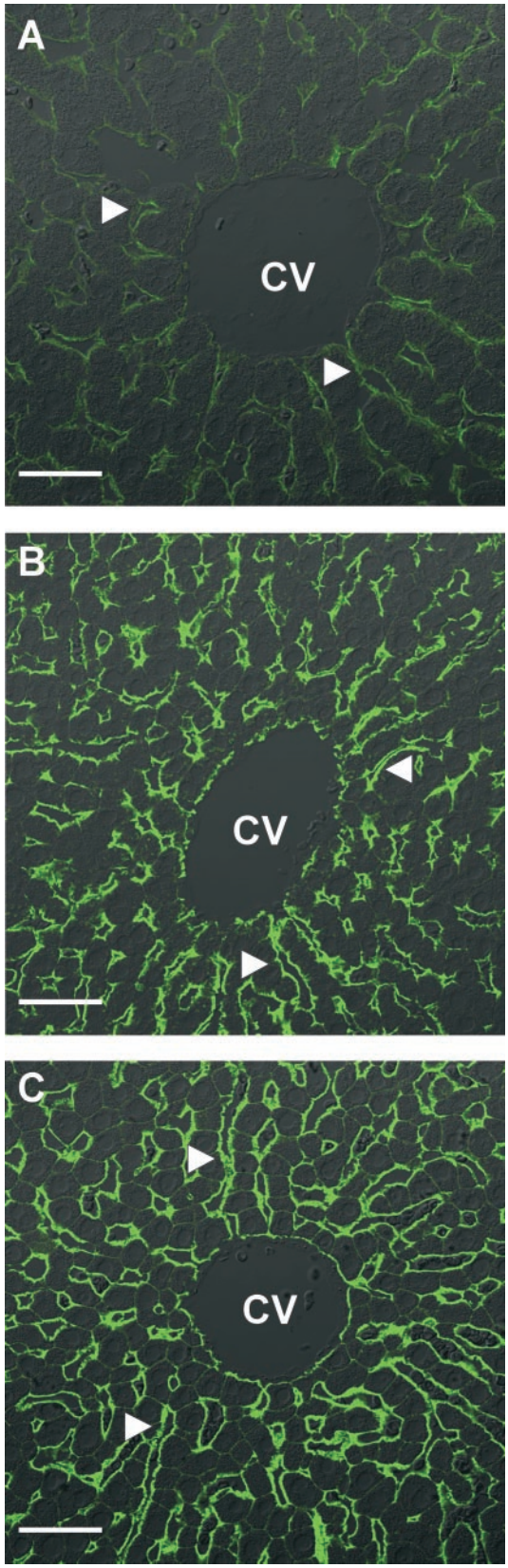

Fig. 5. Confocal laser immunofluorescence microscopy of AQP9 in rat liver. (*A*) Distinct AQP9 immunolabeling is seen associated with hepatocytes in liver from control rat. (*B*) Increased AQP9 immunolabeling associated with hepatocytes close to central vein in liver from rat after 4 days of fasting or (*C*) 9 days after streptozotocin injection. CV, central vein. Arrowheads show sinusoidal surface. Bars indicate 40 μm.

selective channel like AQP4. In contrast, isoosmotic swelling assays confirmed that AQP9 oocytes, but not AQP4 oocytes, transport glycerol. Rates of β-hydroxybutyrate transport were too low to measure accurately. These results were confirmed by measuring uptake of ^{14}C-urea and ^{14}C-glycerol. At pH 7.5, permeability of AQP9 oocytes to ^{14}C-β-hydroxybutyrate was negligible. At pH 5.5 (still above the pKa of 4.7), a modest increase in permeability was detected.

Studies of purified AQP9 protein have not previously been reported. Proteoliposomes reconstituted with purified AQP9 were highly permeable to glycerol and urea, whereas β-hydroxybutyrate permeability was essentially the same as background, and water permeability was only slightly above background (Fig. 2). Thus, AQP9 is much more permeable to glycerol and urea than to water and is essentially impermeable to β-hydroxybutyrate at physiological pH levels.

In vivo studies of AQP9 protein have not previously been reported. Fasting is known to increase blood glycerol levels, and up-regulation of AQP9 was observed in liver as expected. Moreover, AQP9 protein levels continued to rise in liver after fasting up to 96 h, and refeeding caused a gradual return to baseline levels (Fig. 3*C*). During starvation, the liver releases β-hydroxybutyrate and other ketone bodies to substitute for glucose. Kidney and skeletal muscle use ketone bodies but do not express AQP9 (2). Although AQP9 is expressed in brain, fasting-induced changes in protein levels were not observed (not shown).

We investigated other metabolic states known to cause elevations of serum β-hydroxybutyrate or urea; however, levels of AQP9 were not increased in liver. Other urea transporters (18) and β-hydroxybutyrate transporters (19) have been identified in liver; the latter are up-regulated in brain of rats on ketogenic diets (14) and in liver of fasted rats (not shown). The only known mammalian glycerol channels or transporters are aquaporins 3, 7, and 9. AQP7 is not expressed in rat liver (20), and it is not known whether AQP3 is up-regulated in situations where the liver requires increased glycerol import. AQP7 is expressed in adipose tissue (6), where the protein is believed to facilitate the release of glycerol during fasting (21–23). Coordinated regulation of genes encoding mouse AQP7 and AQP9 was recently reported (9). This regulation is thought to maximize glycerol release from adipocytes and glycerol uptake by the liver.

As during fasting, blood insulin levels are low in type 1 diabetes mellitus. Injection of streptozotocin produces a well established animal model of insulin-dependent type 1 diabetes (24). Compared with control rats, streptozotocin-injected rats had elevated blood glucose levels and significantly increased AQP9 protein levels in liver. Treatment of streptozotocin-injected rats with long-acting NPH insulin restored AQP9 to baseline (Fig. 4*B*). One day after administering rapid-acting regular insulin to normal rats, AQP9 levels in the liver decreased 50%, even though blood glucose levels had returned to normal (Fig. 4*A*). These results suggest that insulin represses AQP9 expression *in vivo*.

It is not certain why AQP9 levels are reduced more slowly after refeeding fasted rats than after insulin treatment (compare Figs. 3*C* and 4*A*). In the refed state, insulin levels presumably returned to normal soon after initial refeeding, so it is likely that additional metabolic signals, such as glucocorticoids, may complicate the response. Glucocorticoid levels in the blood increase during fasting and are required for the increased gluconeogenesis in starvation and diabetes (25, 26). In cultured hepatoma cells, dexamethasone increased expression of AQP9, whereas insulin and dexamethasone added together had little effect on AQP9 protein levels (not shown). The human AQP9 promoter contains a glucocorticoid receptor binding motif (27), but it is not known whether elevated glucocorticoid levels persist proportionally longer after longer fasts.

Glycerol is not normally an important gluconeogenic precursor for humans after overnight fasting, but after fasting human

subjects for up to 3.5 days, as much as 21% of circulating glucose is derived from glycerol (28), and fasted rodents have even higher values of circulating glycerol (29, 30). Taken together, recently published studies of AQP9 mRNA (9) and our studies of AQP9 protein strongly support the role for AQP9 expression in liver as a molecular mechanism for maximizing glycerol influx and urea efflux during states requiring increased gluconeogenesis.

We thank M. Daniel Lane and Nicholas F. LaRusso for critical readings of the manuscript, Visvanathan Chandramouli for helpful discussions, and Ida Maria Jalk, Birgit Bonefeld, Weidong Wang, and Lynn Wachtman for assistance. This work was supported in part by grants from the U.S. Public Health Service, National Institutes of Health, the Human Frontier Science Program, the National Danish Research Foundation, the Karen Elise Jensen Foundation, and the European Commission (QLK3-CT-2000-0078).

1. Tsukaguchi, H., Shayakul, C., Berger, U. V., Mackenzie, B., Devidas, S., Guggino, W. B., van Hoek, A. N. & Hediger, M. A. (1998) *J. Biol. Chem.* **273,** 24737–24743.
2. Elkjaer, M., Vajda, Z., Nejsum, L. N., Kwon, T., Jensen, U. B., Amiry-Moghaddam, M., Frokiaer, J. & Nielsen, S. (2000) *Biochem. Biophys. Res. Commun.* **276,** 1118–1128.
3. Nihei, K., Koyama, Y., Tani, T., Yaoita, E., Ohshiro, K., Adhikary, L. P., Kurosaki, I., Shirai, Y., Hatakeyama, K. & Yamamoto, T. (2001) *Arch. Histol. Cytol.* **64,** 81–88.
4. Nicchia, G. P., Frigeri, A., Nico, B., Ribatti, D. & Svelto, M. (2001) *J. Histochem. Cytochem.* **49,** 1547–1556.
5. Ishibashi, K., Sasaki, S., Fushimi, K., Uchida, S., Kuwahara, M., Saito, H., Furukawa, T., Nakajima, K., Yamaguchi, Y., Gojobori, T., *et al.* (1994) *Proc. Natl. Acad. Sci. USA* **91,** 6269–6273.
6. Kuriyama, H., Kawamoto, S., Ishida, N., Ohno, I., Mita, S., Matsuzawa, Y., Matsubara, K. & Okubo, K. (1997) *Biochem. Biophys. Res. Commun.* **241,** 53–58.
7. Agre, P., Bonhivers, M. & Borgnia, M. J. (1998) *J. Biol. Chem.* **273,** 14659–14662.
8. Ko, S. B., Uchida, S., Naruse, S., Kuwahara, M., Ishibashi, K., Marumo, F., Hayakawa, T. & Sasaki, S. (1999) *Biochem. Mol. Biol. Int.* **47,** 309–318.
9. Kuriyama, H., Shimomura, I., Kishida, K., Kondo, H., Furuyama, N., Nishizawa, H., Maeda, N., Matsuda, M., Nagaretani, H., Kihara, S., *et al.* (2002) *Diabetes* **51,** 2915–2921.
10. Sambrook, J., Fritsch, E. F. & Maniatis, T. (1989) *Molecular Cloning: A Laboratory Manual* (Cold Spring Harbor Lab. Press, Plainview, NY), 2nd Ed.
11. Preston, G. M., Carroll, T. P., Guggino, W. B. & Agre, P. (1992) *Science* **256,** 385–387.
12. Saparov, S. M., Kozono, D., Rothe, U., Agre, P. & Pohl, P. (2001) *J. Biol. Chem.* **276,** 31515–31520.
13. Borgnia, M. J. & Agre, P. (2001) *Proc. Natl. Acad. Sci. USA* **98,** 2888–2893.
14. Leino, R. L., Gerhart, D. Z., Duelli, R., Enerson, B. E. & Drewes, L. R. (2001) *Neurochem. Int.* **38,** 519–527.
15. Neely, J. D., Christensen, B. M., Nielsen, S. & Agre, P. (1999) *Biochemistry* **38,** 11156–11163.
16. Laemmli, U. K. (1970) *Nature* **227,** 680–685.
17. Vajda, Z., Pedersen, M., Fuchtbauer, E. M., Wertz, K., Stodkilde-Jorgensen, H., Sulyok, E., Doczi, T., Neely, J. D., Agre, P., Frokiaer, J., *et al.* (2002) *Proc. Natl. Acad. Sci. USA* **99,** 13131–13136.
18. Smith, C. P. & Rousselet, G. (2001) *J. Membr. Biol.* **183,** 1–14.
19. Halestrap, A. P. & Price, N. T. (1999) *Biochem. J.* **343,** 281–299.
20. Ishibashi, K., Kuwahara, M., Gu, Y., Kageyama, Y., Tohsaka, A., Suzuki, F., Marumo, F. & Sasaki, S. (1997) *J. Biol. Chem.* **272,** 20782–20786.
21. Kishida, K., Shimomura, I., Kondo, H., Kuriyama, H., Makino, Y., Nishizawa, H., Maeda, N., Matsuda, M., Ouchi, N., Kihara, S., *et al.* (2001) *J. Biol. Chem.* **276,** 36251–36260.
22. Kishida, K., Kuriyama, H., Funahashi, T., Shimomura, I., Kihara, S., Ouchi, N., Nishida, M., Nishizawa, H., Matsuda, M., Takahashi, M., *et al.* (2000) *J. Biol. Chem.* **275,** 20896–20902.
23. Kondo, H., Shimomura, I., Kishida, K., Kuriyama, H., Makino, Y., Nishizawa, H., Matsuda, M., Maeda, N., Nagaretani, H., Kihara, S., *et al.* (2002) *Eur. J. Biochem.* **269,** 1814–1826.
24. Haughton, C. L., Dillehay, D. L. & Phillips, L. S. (1999) *Lab. Anim. Sci.* **49,** 639–644.
25. Exton, J. H. (1979) *Monogr. Endocrinol.* **12,** 535–546.
26. Gabbay, R. A., Sutherland, C., Gnudi, L., Kahn, B. B., O'Brien, R. M., Granner, D. K. & Flier, J. S. (1996) *J. Biol. Chem.* **271,** 1890–1897.
27. Tsukaguchi, H., Weremowicz, S., Morton, C. C. & Hediger, M. A. (1999) *Am. J. Physiol.* **277,** F685–F696.
28. Baba, H., Zhang, X. J. & Wolfe, R. R. (1995) *Nutrition* **11,** 149–153.
29. Peroni, O., Large, V., Odeon, M. & Beylot, M. (1996) *Metabolism* **45,** 897–901.
30. Peroni, O., Large, V. & Beylot, M. (1995) *Am. J. Physiol.* **269,** E516–E523.